

# Antiferroquadrupolar Order in the Magnetic Semiconductor TmTe

Jean-Michel MIGNOT, Arsen GUKASOV, Changping YANG, Peter LINK\*, Takeshi MATSUMURA<sup>1</sup>  
and Takashi SUZUKI<sup>2</sup>

*Laboratoire Léon Brillouin, CEA-CNRS, CEA/Saclay, F-91191 Gif sur Yvette, France*

<sup>1</sup>*Department of Physics, Tohoku University, Sendai 980-77, Japan*

<sup>2</sup>*National Research Institute for Metals, Tsukuba, Ibaraki 305-0047, Japan*

The physical properties of the antiferroquadrupolar state occurring in TmTe below  $T_Q = 1.8$  K have been studied using neutron diffraction in applied magnetic fields. A field-induced antiferromagnetic component ( $\mathbf{k} = (\frac{1}{2}, \frac{1}{2}, \frac{1}{2})$ ) is observed and, from its magnitude and direction for different orientations of  $H$ , an  $O_2^2$  quadrupole order parameter is inferred. Measurements below  $T_N \approx 0.5$  K reveal that the magnetic structure is canted, in agreement with theoretical predictions for in-plane antiferromagnetism. Complex domain repopulation effects occur when the field is increased in the ordered phases, with discontinuities in the superstructure peak intensities above 4 T.

KEYWORDS: quadrupole order, antiferroquadrupolar, antiferromagnetic, neutron diffraction, TmTe

## §1. Introduction

The number of experimental studies devoted to orbital phenomena in magnetic materials has grown rapidly during the last five years. Long-range order involving orbital degrees of freedom has now been reported for a broad range of materials, from transition-metal oxides ( $V_2O_3$ ,  $LaMnO_3$ , etc.) to rare-earth or actinide compounds. In contrast to  $3d$  elements, lanthanide ions are characterized by a strong coupling between the total spin and orbital momenta, which rules out pure orbital order. Charge order, an important issue in manganites, is also not relevant for “normal” rare-earth compounds because the occupancy of the  $4f$  shell has a fixed integral value. On the other hand, it has long been recognized<sup>1,2</sup>) that interactions between multipole moments of the  $f$ -electron wavefunctions — especially the quadrupole (QP) moments representing the asphericity of the charge distribution — can play a significant role at low temperature, and even lead to a phase transition into a long-range ordered state.<sup>3</sup>) In analogy with magnetic systems, this state is termed “ferroquadrupolar” when the order parameter is uniform, “antiferroquadrupolar” (AFQ) when its periodicity differs from that of the lattice.<sup>4</sup>)

A few members of the second class have been known for as much as 20 years ( $CeB_6$ ,<sup>5</sup>)  $PrPb_3$ <sup>6</sup>), but more examples have been discovered recently ( $DyB_2C_2$ <sup>7</sup>) as a result of an intensive experimental effort using a broad spectrum of techniques. The fingerprint of the AFQ transition may be elusive in the magnetic susceptibility,<sup>8</sup>) but clear anomalies are observed in the specific heat<sup>5,8</sup>) or the elastic constants.<sup>8,9</sup>) In most cases, the complexity arising from the tensor character of the QP moment operator can be disentangled only through single-crystal

diffraction measurements.

In this context, x-ray scattering has the unique advantage that it can probe the asphericity of the  $4f$  charge distribution without the need to apply a magnetic field. AFQ order was detected recently by this technique in several compounds ( $NdMg$ ,<sup>10</sup>)  $CeB_6$ ,<sup>11,12</sup>)  $UPd_3$ ,<sup>13</sup>)  $DyB_2C_2$ <sup>14,15</sup>). However, such experiments are not straightforward because the measured intensities are very weak in the case of conventional Thomson scattering, and those obtained in resonant experiments are difficult to interpret quantitatively. Neutrons, which have no direct interaction with QP moments, can nonetheless disclose the “hidden” QP order through its effect on the magnetic response to an applied magnetic field. This was first demonstrated in the case of  $CeB_6$  by Effantin *et al.*,<sup>16</sup>) who observed field-induced antiferromagnetic (AFM) peaks below the transition temperature  $T_Q$ , reflecting the existence of distinct easy axes on the two AFQ sublattices. That strategy also proved quite successful with TmTe, as reported below. Furthermore, neutrons provide an ideal tool to study the magnetic order which sets in at lower temperature and the interplay between the QP and dipole order parameters.

TmTe is a cubic, NaCl structure, magnetic semiconductor with an energy gap of about 0.35 eV.<sup>17</sup>) Tm ions are divalent ( $4f^{13}$ ), and the ground-state multiplet  $^2F_{7/2}$  is split by the crystal field into one quartet ( $\Gamma_8$ ) and two Kramers doublets ( $\Gamma_7$ ) and ( $\Gamma_6$ ). Neutron scattering results<sup>18</sup>) indicate that the overall splitting is quite small (about 1 meV) and that the ground state is most likely  $\Gamma_8$ , as proposed previously from elastic constant and thermal expansion measurements.<sup>19,20</sup>) AFQ order, with a transition temperature of  $T_Q = 1.8$  K was discovered by Matsumura *et al.*,<sup>8,21</sup>) using specific heat and ultrasonic experiments. The study of QP interactions in this system is of particular interest because, unlike intermetallic compounds such as  $CeB_6$  or  $PrPb_3$ , TmTe has a very low carrier concentration at temperatures of

\* Present address: Inst. für Physikalische Chemie, Universität Göttingen, Tammannstr. 6, Göttingen, Germany.

the order of  $T_Q$ , and the role of interactions mediated by conduction electrons<sup>22)</sup> can be considered negligible. On the other hand, no sizeable lattice distortion indicative of magnetoelastic couplings could be detected so far. AFM order was reported to occur with a transition temperature  $T_N$  comprised between 0.23 K (magnetic susceptibility<sup>8,23,24)</sup> and 0.43 K (neutron diffraction).<sup>25)</sup>

In the following, we report a detailed study of the AFQ and AFM phases of TmTe by neutron diffraction. Section 3.1 presents the observation of the field-induced AFM superstructure below  $T_Q$ , and the analysis of the data for different field directions, leading to the identification of the order parameter. These results have been described in more detail in previous publications.<sup>26–29)</sup> Next we set out to discuss the magnetic transition and the dipole-ordered phase occurring below  $T_N$ . Recent measurements carried out down to 100 mK are reported in Section 3.2. They reveal the existence of a canting of the magnetic structure which can be regarded as the consequence of QP order. The application of large magnetic fields at very low temperature produce domain reorientation phenomena with dramatic irreversibilities. The final section outlines possible directions for future studies on this system.

## §2. Experiments

To observe QP order in TmTe and determine its phase diagram, it is necessary to apply large magnetic fields and to cool the sample down to  $T < T_Q = 1.8$  K. Even lower temperatures are required for studying the transition into the AFM phase. These conditions were achieved by using two different split-coil, vertical field cryomagnets with maximum fields of 7.5 and 12 T, respectively. The former could be equipped with a <sup>3</sup>He-<sup>4</sup>He dilution insert yielding a minimum mixing-chamber temperature of about 100 mK. Thermal coupling of the sample to the cold plate carrying the temperature sensors was ensured by a gold wire, which proved to be effective down to about 150 mK.

Neutron diffraction experiments were carried out on the two-axis lifting-counter diffractometers 6T2 (thermal beam) and 5C1 (hot source) at the Orphée reactor in Saclay. Measurements were made at neutron wavelengths of 0.90 or 2.35 Å (6T2), and 0.84 Å (5C1) with a primary beam collimation of 50'. Second-order contaminations were suppressed by means of erbium or pyrolytic graphite filters. For the polarized-neutron experiments, 5C1 was operated with a Heusler-alloy monochromator, providing a polarization  $P_0 = 0.91$  at 0.84 Å.

Measurements were taken on a large TmTe single crystal (lattice constant  $a_0 = 6.354$  Å), prepared by induction-melting of high-purity constituents inside a vacuum-sealed tungsten crucible.<sup>8)</sup> From its lattice constant, as well as from polarized-neutron results reported previously,<sup>27)</sup> this sample was concluded to be close to stoichiometric, with an estimated Tm deficiency of  $0.04 \pm 0.01$ . Different orientations of the crystal with respect to the magnetic field ( $\mathbf{H} \parallel [110]$ ,  $[001]$  and  $[111]$ ) were studied in separate experiments.

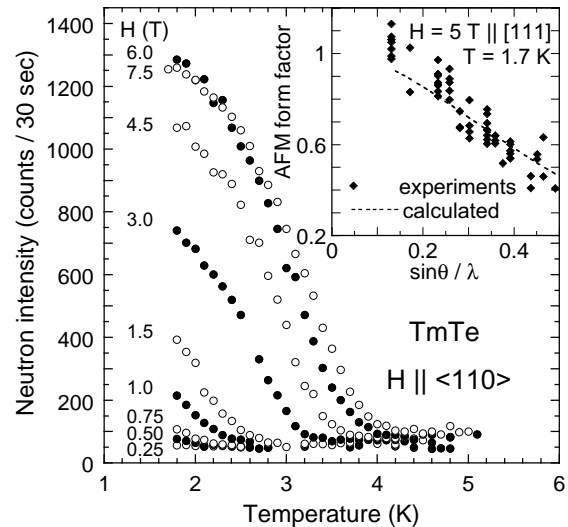


Fig. 1. Intensity of the field-induced magnetic Bragg peak  $\frac{1}{2}\frac{1}{2}\frac{1}{2}$  as a function of temperature for different magnetic fields applied along  $[110]$ . Inset: magnetic form factor associated with the induced AFM reflections measured at  $T = 1.7$  K in a field of 5 T along  $[111]$ ; the dashed line represents the  $\text{Tm}^{2+}$  form factor calculated in the dipolar approximation.

## §3. Results

### 3.1 Antiferroquadrupolar order

When TmTe is cooled in an applied magnetic field, superstructure peaks corresponding to the wave vector  $\mathbf{k} = (\frac{1}{2}, \frac{1}{2}, \frac{1}{2})$  (type-II AFM) appear below the critical temperature  $T_Q$ . Intensities measured with  $\mathbf{H} \parallel [110]$  are shown in Fig. 1 for different field values. The reflections vanish for  $H = 0$ , which indicates that the transition occurring in zero field is not associated with magnetic dipole order. On the other hand, the  $\mathbf{Q}$  dependence of the field-induced intensities approximately follows that calculated for the  $\text{Tm}^{2+}$  magnetic form factor (inset in Fig. 1). Therefore the observed superstructure results from magnetic scattering and cannot be ascribed to a distortion of the lattice, which would at any rate require unphysically large atomic displacements to account for the experimental peak intensities. The observation of a staggered magnetic response in a uniform applied field is explained naturally by assuming that the transition at  $T_Q$  corresponds to the ordering of  $4f$  QP moments in a long-range structure with the wave vector  $(\frac{1}{2}, \frac{1}{2}, \frac{1}{2})$ , which splits the Tm sites into two sublattices with different local anisotropy axes. Similar results have been obtained for  $\mathbf{H} \parallel [111]$ . For  $\mathbf{H} \parallel [001]$  extra peaks are also observed but their intensities are much weaker. Phase diagrams drawn from the neutron data for the three field directions are in general agreement with those derived previously from the specific heat. In particular, the critical temperature is strongly enhanced by the external field for all symmetry directions, and the QP transition line closes up above 5 T for  $\mathbf{H} \parallel [001]$ .

To obtain more detailed information on the AFQ order we have refined the induced AFM structure for  $\mathbf{H} \parallel [110]$  and  $\mathbf{H} \parallel [111]$ . For both orientations, the AFM Fourier component  $\mathbf{m}_{\mathbf{k}}$  was found to be directed along one of the three two-fold cubic axes perpendicular to the wave vector  $\mathbf{k}$ . This gives rise to three possible magnetic do-

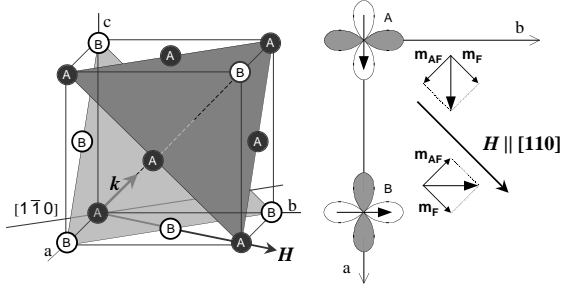


Fig. 2. Schematic representation of the AFQ structure showing the A and B sublattices associated with the wave vector  $\mathbf{k}_1$  (left), and the field-induced uniform ( $\mathbf{m}_F$ ) and staggered ( $\mathbf{m}_{AF}$ ) components for  $\mathbf{H} \parallel [110]$  (right).

mains, denoted “*S*-domains”, whose populations can be derived from the refinement. From the field dependence of the  $k$ -domain populations (see below) the structure is expected to be single- $\mathbf{k}$ , and the the AFM moment on the Tm sublattices is thus equal to  $\pm \mathbf{m}_k$ . The resulting structure for  $\mathbf{H} \parallel [110]$  is represented in Fig. 2 for the wave vector  $(\frac{1}{2}, \frac{1}{2}, \frac{1}{2})$ . The AFM component ( $\mathbf{m}_k = 1.6 \mu_B$  for  $H = 5$  T) is drawn perpendicular to both  $\mathbf{H}$  and  $\mathbf{k}$  because this corresponds to the *S*-domain found to prevail in high fields. Also shown is the uniform magnetic component along  $\mathbf{H}$  ( $\mathbf{m}_0 = 2.60(3) \mu_B$  for  $H = 4$  T from the polarized-neutron results). For  $\mathbf{H} \parallel [001]$ , a similar refinement was not possible because the experimental intensities were not strong enough.

Using the symmetry relations between the AFQ order parameter and the field-induced dipole moments derived previously for CeB<sub>6</sub>,<sup>30)</sup> it can be inferred from the above results that the primary QP order parameter is most likely  $O_2^{26)$ . A detailed study of multipole interactions in TmTe has been carried out by Shiina *et al.*<sup>31)</sup> using a classical mean-field model, in which the Tm sites are considered to form four uncoupled simple-cubic (*sc*) sublattices. Their results indeed confirm that, if the crystal field is chosen with an easy axis along [001], the experimental data can be explained consistently in terms of a  $\Gamma_3$  (tetragonal) QP order parameter. The situation for  $\mathbf{H} \parallel [110]$  is depicted schematically in Fig. 2.

The variations of the AFM peak intensities with the external field reveal interesting domain repopulation effects. In low fields, the four different  $k$ -domains, associated with the wave vectors  $\mathbf{k}_1 = (\frac{1}{2}, \frac{1}{2}, \frac{1}{2})$ ,  $\mathbf{k}_2 = (\frac{1}{2}, \frac{1}{2}, -\frac{1}{2})$ ,  $\mathbf{k}_3 = (\frac{1}{2}, -\frac{1}{2}, \frac{1}{2})$  and  $\mathbf{k}_4 = (-\frac{1}{2}, \frac{1}{2}, \frac{1}{2})$  are found to exist. If  $H$  is increased along [111], one single domain, corresponding to  $\mathbf{k}_1 \parallel \mathbf{H}$ , grows at the expense of the other three. This behavior implies that the structure is single- $\mathbf{k}$ . A different situation exists for  $\mathbf{H} \parallel [110]$  as *two* domains,  $\mathbf{k}_1 = (\frac{1}{2}, \frac{1}{2}, \frac{1}{2})$  and  $\mathbf{k}_2 = (\frac{1}{2}, \frac{1}{2}, -\frac{1}{2})$ , are favored in high fields (Fig. 3). As in the previous case, the dominant domains turn out to be those whose  $\mathbf{k}$  vector makes the smallest angle (35 degrees) with the external field. The above model,<sup>31)</sup> completed by introducing an additional electrostatic QP-QP coupling between the *sc* sublattices,<sup>32)</sup> correctly predicts the single- $\mathbf{k}$  structure, as well as the domain repopulation for  $\mathbf{H} \parallel [111]$ , but not that for  $\mathbf{H} \parallel [110]$ . A more realistic treatment of these interactions appears to be necessary.

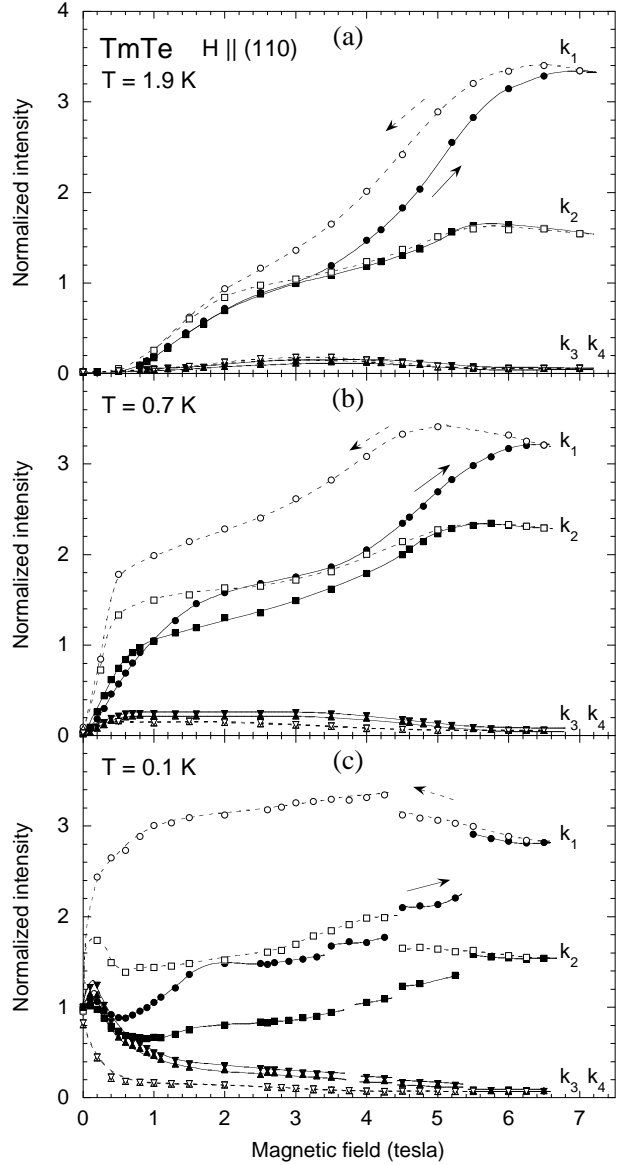


Fig. 3. Intensities of the magnetic peaks  $\pm \frac{1}{2} \pm \frac{1}{2} \pm \frac{1}{2}$  associated with the four  $k$ -domains  $\mathbf{k}_1 \dots \mathbf{k}_4$  as a function of the applied field  $H \parallel [110]$ , measured in the AFQ (a, b) and AFM (c) phases. Closed (open) symbols denote measurements taken on increasing (decreasing)  $H$ . Data for each  $\mathbf{k}$  vector have been normalized to the zero-field value at  $T = 0.1$  K (see Section 3.2).

The field dependences ( $\mathbf{H} \parallel [110]$ ) of the induced intensities of  $\pm \frac{1}{2} \pm \frac{1}{2} \pm \frac{1}{2}$  reflections corresponding to the four  $k$ -domains are plotted in Figs. 3a and 3b for two temperatures within the AFQ phase. At  $T = 1.9$  K the zero-field state is paramagnetic and the AFM signal therefore appears only above a threshold at about 0.5 T. At  $T = 0.7$  K, on the other hand, the intensity increases steeply from  $H = 0$ . In both cases the variation takes place in two steps, and the intensities from the depleted domains  $\mathbf{k}_3$  and  $\mathbf{k}_4$  start to decrease only above 3.5 T, in connection with a pronounced upturn in those from the dominant domains. As a result, a sizeable AFM component is induced even in the minority domains before the  $k$ -domain repopulation is completed. Another point to be noted is that the intensities associated with  $\mathbf{k}_1$  and  $\mathbf{k}_2$  differ significantly in large fields, especially at  $T = 1.9$  K, presumably because a small deviation

from the nominal sample orientation with respect to the field makes these domains not strictly equivalent. In contrast, their variations remain very similar up to 3 T. A double- $\mathbf{k}$  to single- $\mathbf{k}$  transition could produce this type of behavior, but it seems incompatible with the domain repopulation observed for  $\mathbf{H} \parallel [111]$ . Another possibility is that the  $k$ -domains essentially retain their initial populations up to 3 T, and that the difference between the two types of domains reflects their intrinsic staggered response in the applied field. Detailed data collections and structure refinements at several values of  $H$  should be conducted to clarify this point. As could be expected, large irreversibilities at increasing and decreasing field are observed in connection with the changes in domain populations. This effect becomes more pronounced at lower temperature.

### 3.2 Dipole moment order

Various experimental results indicate that a second phase transition corresponding to the ordering of the Tm dipole moments, takes place at  $T_N \ll T_Q$ .<sup>8,23-25)</sup> The magnetic structure was identified as type-II AFM from the observation of neutron Bragg peaks associated with the wave vector  $\mathbf{k} = (\frac{1}{2}, \frac{1}{2}, \frac{1}{2})$ .<sup>25)</sup> At the time that result was reported, the existence of AFQ order was not suspected and it was therefore natural to assume the magnetic structure to be conventional AFII. However, the mean-field theory<sup>31)</sup> suggests that the AFQ order should have sizeable effects on the magnetic phase transition: it is expected to favor FM correlations, thereby causing a substantial reduction of  $T_N$  and, in the case of “in-plane” AFM order (ordered dipole moments lying within the plane of the  $O_2^2$  quadrupoles) which seems appropriate for TmTe, to produce a canting of the AFM structure. This canting consists in the rotation of the dipole moments on each sublattice by  $+\phi$  and  $-\phi$  respectively with respect to the local anisotropy axis, and should be observable experimentally.

Our measurements for  $H = 0$  confirm the existence of AFII magnetic Bragg peaks. In the upper frame of Fig. 4, the integrated intensity of the  $\frac{1}{2}\frac{1}{2}\frac{1}{2}$  reflection is plotted as a function of  $T$ , together with the previous results of Lassailly *et al.*<sup>25)</sup> Despite the use of crystals from different origins, the agreement between the two sets of data is excellent. A tendency to saturation is observed in our measurements below 0.15 K, probably due to insufficient thermalization of the sample exposed to the neutron beam. One notes that the magnetic intensity persists far above the Néel temperature  $T_N = 0.45$  K reported in ref. 25. However, the sharp maximum in the  $T$  dependence of the Bragg peak *width* on which the latter estimate was based could not be reproduced in the present experiments. Our data merely indicate a moderate monotonic broadening of the rocking curves accompanying the intensity drop as the system is heated up to 0.6 K. The determination of  $T_N$  from the neutron intensities thus remains elusive. We recall that similar difficulties were also encountered with other techniques, as the ac susceptibility<sup>8,23,24)</sup> shows a divergence at 0.22 K but no anomaly around 0.5 K, and the specific-heat peak corresponding to the AFM transition exhibits a complex

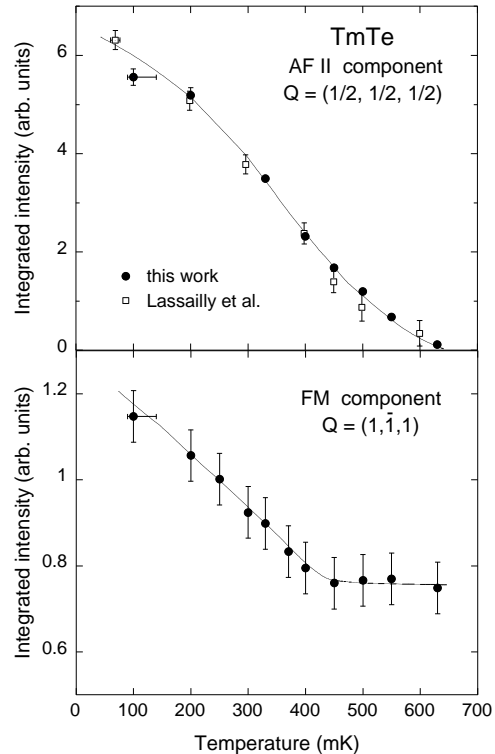


Fig. 4. Integrated intensities of the  $\frac{1}{2}\frac{1}{2}\frac{1}{2}$  (AFM) and  $1\bar{1}1$  (FM) peaks measured in zero field as a function of temperature. The data of ref. 25 are plotted in the upper frame for comparison.

structure with a peak at 0.34 K followed by a shoulder near 0.5 K.<sup>8)</sup> These problems may reflect the existence of anomalously strong fluctuations, which have been predicted to occur because of competing interactions between different multipole moments.

The lower frame in Fig. 4 represents the integrated intensity of the weak  $1\bar{1}1$  nuclear peak as a function of temperature. The increase observed below 0.45 K clearly demonstrates that a superimposed ferromagnetic component develops below  $T_N$  in addition to the AFM superstructure, with a magnitude of about  $0.4 \mu_B$ , as compared to  $2.3 \mu_B$  for the AFM component. The observation of this canting component lends additional support to the model of ref. 31. Within the limited accuracy of the measurement, no significant magnetic signal seems to remain above 0.45 K, in contrast to the AFM component.

Indications as to the dimensions of the magnetic domains can be derived from an analysis of the width of the  $1\bar{1}1$  reflection. At  $T = 0.55$  K in zero field, the intensity is purely nuclear and the width of the rocking curve thus reflects the experimental resolution and the mosaic of the crystal. For  $T = 0.1$  K, the magnetic intensities were obtained by subtracting out this nuclear signal. The results for  $H = 0$  and 6.5 T are plotted in Fig. 5, together with the nuclear peak. For the sake of comparison, all curves have been normalized because their intensities differ by orders of magnitude (nucl:FM[ $H = 0$ ]:FM[6.5 T]  $\approx 5:1:150$ ). The graph clearly shows that the magnetic peak in zero field is substantially broader than the resolution. This effect can be ascribed to a finite correlation length  $\xi$  of the FM component, estimated to be of the order of 50 Å, which probably reflects the existence of

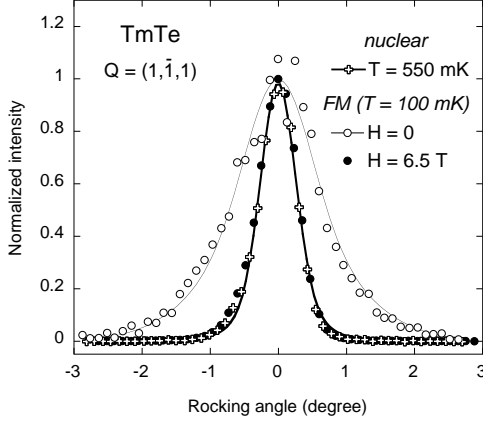


Fig. 5. Normalized rocking curves through the  $\bar{1}\bar{1}1$  reflection. Crosses and thick lines: nuclear contribution with Gaussian fit; open circles and thin line: zero-field FM component with Gaussian fit; closed circles: high-field FM component.

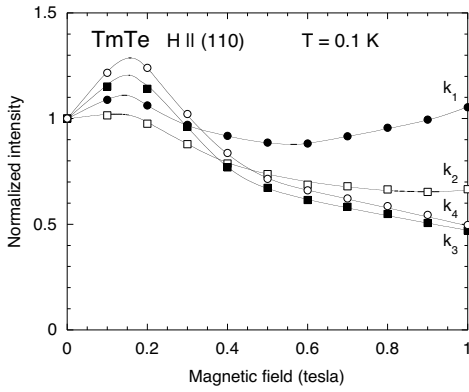


Fig. 6. Intensities of the magnetic peaks  $\pm\frac{1}{2}\pm\frac{1}{2}\pm\frac{1}{2}\pm\frac{1}{2}$  associated with the four  $k$ -domains  $k_1 \dots k_4$  as a function of the applied field  $H \parallel [110]$ , measured in the AFM phase (expanded plot of the low-field part of Fig. 3c).

magnetic domains with different directions of canting. In contrast, the FM component measured at 6.5 T can be superimposed almost perfectly on the nuclear peak, implying that  $\xi$  becomes infinite (to the precision of the measurement) when the field becomes large enough to reorient the domains. This effect takes place at relatively low fields, as a narrow peak is already recovered at  $H = 2$  T.

The field dependences ( $H \parallel [110]$ ) of the AFM peak intensities for  $T \approx 0.1$  K  $< T_N$  is displayed in Fig. 3c. In contrast to the data for  $T > T_N$  plotted in frames a and b, finite intensities exist already in zero field because the wave vectors of the AFM and AFQ ordered states are the same. The measured values are different for  $k_1$  and  $k_2$  on the one hand,  $k_3$  and  $k_4$  on the other hand, owing to different scattering geometries (Lorentz factor and resolution). However, it was checked by comparing integrated intensities for different sets of equivalent reflections that the zero-field populations of the four  $k$ -domains do not differ significantly. The curves in Fig. 3c were thus normalized to the same value for  $H = 0$ , and the same scaling factor was also applied to the corresponding data plotted in the other two frames.

One can roughly distinguish three different regimes as a function of the applied field. Below 1 T (Fig. 6),

a general decrease in the AFM intensity takes place, with initially a weak maximum near 0.15 T for  $k_3$  and  $k_4$ . This region is dominated by dipole moment order and may involve some reorientation among  $S$ -domains. Such a view is consistent with the specific-heat results, in which a magnetic-ordering anomaly could be traced up to  $H \approx 1$  T. At higher fields, the intensities for the  $k_1$  and  $k_2$  domains go through a minimum and start to increase. The situation resembles that observed at  $T = 0.7$  K, *i.e.* for pure AFQ order. However, for fields in excess of 3 T, one observes a succession of jumps, with a positive sign for  $k_1$  and  $k_2$ , a negative sign and a smaller magnitude for  $k_3$  and  $k_4$ . Similar discontinuities, known as “Barkhausen steps” are commonly observed in the magnetization curves of ferromagnets. They originate from random irreversible domain-wall jumps as  $H$  is increased. In Section 3.1, it was indeed suggested that most of the repopulation of AFQ domains takes place in the range  $H > 3$  T. The observation of such a behavior in an AFM phase is quite interesting and calls for further investigations. Surprisingly, no anomalies have been detected in the bulk magnetization for this field direction.<sup>24)</sup> How domain reorientation responsible for sizeable jumps in the AFM field-induced component can have no fingerprint in the uniform component thus remains to be explained.

#### §4. Conclusions

The results obtained in the present work provide a comprehensive picture of ordering phenomena in TmTe, involving both dipole and QP moments. Qualitative agreement is found with the main predictions of a mean-field model based on a classical treatment of crystal-field, quadrupolar and exchange interactions. In particular, the canting of the magnetic moments anticipated for in-plane AFM order is observed experimentally below  $T_N$ . On the other hand, a number of questions remain open. Probably the most important one concerns the nature of QP interactions in TmTe. As noted at the outset, the conduction-electron-mediated, RKKY-type, mechanism<sup>22)</sup> proposed for intermetallic compounds is not applicable here. Alternative possibilities are a coupling through the lattice, as in Jahn-Teller insulators,<sup>33)</sup> or a superexchange-like interaction between Tm next nearest neighbors separated by one Te atom as proposed in ref. 31. Experimentally, it is not simple to distinguish between those mechanisms: in particular, it has been argued that AFQ order itself should result in sizeable lattice distortions below  $T_Q$ .<sup>34)</sup> High-resolution x-ray diffraction experiments should be performed to clarify this point. Resonant experiments could also allow the AFQ order to be probed directly in zero field. This requires, however, to reach temperatures of less than 1.8 K, and to obtain crystals with very small mosaic spread.

Our present interpretation of the AFQ phase as due to an  $O_2^2$  QP order parameter seems consistent with the bulk of experimental observations, but some points require further examination. In particular, the results for  $H \parallel [001]$  are not well understood, mainly because of the weakness of the signals. Even so, the fact that a finite induced AFM component exists seems in contradiction

with the symmetry arguments of Shiina *et al.*<sup>30)</sup> which predict that component to vanish. This may indicate that the latter analysis, initially performed for CeB<sub>6</sub> (*sc*) is not readily applicable to *fcc* TmTe because the small groups of the  $\mathbf{k}$  vector ( $\frac{1}{2}, \frac{1}{2}, \frac{1}{2}$ ) for the two types of Bravais lattices are different.<sup>35)</sup> It was also predicted that for this field direction, the external field should stabilize the component  $O_2^0$  with respect to  $O_2^2$ , possibly causing a transition between two AFQ phases.<sup>31)</sup> Experimental evidence for such a transition is still lacking but it has been suggested that it might be responsible for the steplike jump observed in the bulk magnetization for  $\mathbf{H} \parallel [001]$  at very low temperature.<sup>24)</sup> As to the properties of the AFM state, the results reported in this paper reveal quite interesting behaviors, especially in strong applied magnetic fields. Additional experiments are required to work out a reliable refinement of the magnetic structure in the presence of complex domain reorientation effects.

### Acknowledgements

We thank Th. Beaufils, Ph. Boutrouille and P. Fouilloux for help with the experiments, R. Shiina for numerous comments and suggestions, and A. V. Nikolaev, H. Shiba and O. Sakai for useful discussions.

- 
- 1) M. Blume and Y. Y. Hsieh: *J. Appl. Phys.* **40** (1969) 1249.
  - 2) J. Sivardière and M. Blume: *Phys. Rev. B* **5** (1972) 1126.
  - 3) P. Morin and D. Schmitt: *Ferromagnetic Materials*, ed. K. H. J. Buschow and E. P. Wohlfarth (North-Holland 1990) p. 1.
  - 4) Strictly speaking, one should distinguish between different types of non-uniform QP structure (commensurate / incommensurate, single- / multi- $\mathbf{k}$ , collinear / noncollinear). However, experimental evidence is so far lacking for the occurrence of such situations in real systems.
  - 5) Y. Peysson, C. Ayache, J. Rossat-Mignod, S. Kunii and T. Kasuya: *J. Phys. (France)* **47** (1986) 113.
  - 6) E. Bucher, K. Andres, A. C. Gossard and J. P. Maita: *Proceedings of the 13th Conference on Low Temperature Physics, LT 13*, ed. K. D. Timmerhaus, W. J. O'Sullivan and E. F. Hammel (Plenum Publishing Corp., New York 1974) p. 322.
  - 7) H. Yamauchi, H. Onodera, K. Ohoyama, T. Onimaru, M. Kosaka, M. Ohashi and Y. Yamaguchi: *J. Phys. Soc. Jpn.* **68** (1999) 2057.
  - 8) T. Matsumura, S. Nakamura, T. Goto, H. Amitsuka, K. Matsuhira, T. Sakakibara and T. Suzuki: *J. Phys. Soc. Jpn.* **67** (1998) 612.
  - 9) T. Goto, A. Tamaki, S. Kunii, T. Nakajima, T. Fujimura, T. Kasuya, T. Komatsubara and S. B. Woods: *J. Magn. Magn. Mater.* **31** (1983) 419.
  - 10) M. Amara, R. M. Galéra, P. Morin and J. F. Béar: *J. Phys.: Condens. Matter* **10** (1998) L743.
  - 11) H. Nakao, K. I. Magishi, Y. Wakabayashi, Y. Murakami, K. Koyama, K. Hirota, Y. Endoh and S. Kunii: *J. Phys. Soc. Jpn.* **70** (2001) 1857.
  - 12) F. Yakhov, V. Plakhty, H. Suzuki, S. Gavrilov, P. Burlet, L. Paolasini, C. Vettier and S. Kunii: *Phys. Lett. A* **285** (2001) 191.
  - 13) D. F. McMorrow, K. A. McEwen, U. Steigenberger, H. M. Rnnow and F. Yakhov: *Phys. Rev. Lett.* **87** (2001) 057201/1.
  - 14) K. Hirota, N. Oumi, T. Matsumura, H. Nakao, Y. Wakabayashi, Y. Murakami and Y. Endoh: *Phys. Rev. Lett.* **84** (2000) 2706.
  - 15) Y. Tanaka, T. Inami, T. Nakamura, H. Yamauchi, H. Onodera, K. Ohoyama and Y. Yamaguchi: *J. Phys.: Condens. Matter* **11** (1999) L505.
  - 16) J. M. Effantin, J. Rossat-Mignod, P. Burlet, H. Bartholin, S. Kunii and T. Kasuya: *J. Magn. Magn. Mater.* **47&48** (1985) 145.
  - 17) P. Wachter: *Handbook of the Physics and Chemistry of Rare Earths*, ed. K. A. Gschneider, Jr., L. Eyring, G. H. Lander and G. R. Choppin (Elsevier Science 1994) p. 177, and references therein.
  - 18) E. Clementyev, R. Koehler, M. Braden, J.-M. Mignot, C. Vettier, T. Matsumura and T. Suzuki: *Physica B* **230** (1997) 735.
  - 19) H. R. Ott, B. Lüthi and P. S. Wang: *Valence Instabilities and Related Narrow-Band Phenomena*, ed. R. D. Parks (Plenum Press 1977) p. 289.
  - 20) H. R. Ott and B. Lüthi: *Z. Phys. B* **28** (1977) 141.
  - 21) T. Matsumura, Y. Haga, Y. Nemoto, S. Nakamura, T. Goto and T. Suzuki: *Physica B* **206&207** (1995) 380.
  - 22) P. M. Levy, P. Morin and P. Schmitt: *Phys. Rev. Lett.* **42** (1979) 1417.
  - 23) E. Bucher, K. Andres, F. J. di Salvo, J. P. Maita, A. C. Gossard, A. S. Cooper and G. W. Hull, Jr.: *Phys. Rev. B* **11** (1975) 500.
  - 24) T. Sakakibara, S. Honma, T. Tayama, K. Tenya, H. Amitsuka, T. Matsumura and T. Suzuki: *Physica B* **281** (2000) 566.
  - 25) Y. Lassailly, C. Vettier, F. Holtzberg, A. Benoit and J. Flouquet: *Solid State Commun.* **52** (1984) 717.
  - 26) P. Link, A. Gukasov, J.-M. Mignot, T. Matsumura and T. Suzuki: *Phys. Rev. Lett.* **80** (1998) 4779.
  - 27) P. Link, A. Gukasov, J.-M. Mignot, T. Matsumura and T. Suzuki: *Physica B* **259-261** (1999) 319.
  - 28) P. Link, T. Matsumura, A. Gukasov, J.-M. Mignot and T. Suzuki: *Physica B* **281&282** (2000) 569.
  - 29) J.-M. Mignot, P. Link, A. Gukasov, I. N. Goncharenko, T. Matsumura and T. Suzuki: *Physica B* **281&282** (2000) 470.
  - 30) R. Shiina, H. Shiba and P. Thalmeier: *J. Phys. Soc. Jpn.* **66** (1997) 1741.
  - 31) R. Shiina, H. Shiba and O. Sakai: *J. Phys. Soc. Jpn.* **68** (1999) 2105.
  - 32) R. Shiina, H. Shiba and O. Sakai: *J. Phys. Soc. Jpn.* **68** (1999) 2390.
  - 33) G. A. Gehring and K. A. Gehring: *Rep. Prog. Phys.* **38** (1975) 1.
  - 34) A. V. Nikolaev and K. H. Michel: *Phys. Rev. B* **63** (2001) 104105/1.
  - 35) O. Sakai, private communication.